Encapsulation of cesium with a solid waste-derived sulfoaluminate matrix: a circular economy approach of treating nuclear wastes with solid wastes

Jingwei Li[†], Dong Xu[†], Xujiang Wang[†], Kang Liu[††], Yanpeng Mao[†], Mengmeng Wang[††], Yun Bai[†††], Wenlong Wang[†*]

[†]Shandong Engineering Laboratory for Solid Waste Green Materials, National Engineering Laboratory for Reducing Emissions from Coal Combustion, Engineering Research Center of Environmental Thermal Technology of Ministry of Education, Shandong Key Laboratory of Energy Carbon Reduction and Resource Utilization, School of Energy and Power Engineering, Shandong University, Jinan 250014, China

[††]State Key Joint Laboratory of Environment Simulation and Pollution Control, School of Environment, Tsinghua University, Beijing 100084, China

[†††]Department of Civil, Environmental and Geomatic Engineering, University College London, Gower Street, London, WC1E 6BT, UK

[*] **Corresponding Author**

E-mail address: wwenlong@sdu.edu.cn

Abstract

It is of great importance to safely dispose nuclear wastes with the development of nuclear industries. Past approaches to this problem have included immobilizing radioactive cesium in Portland cement-based matrices; however, the leaching rates of cesium are relatively high, especially as the leaching temperature increases. This paper explores a high-efficiency and cost-effective approach for encapsulating cesium using a sulfoaluminate cement (SAC) matrix, which was prepared *via* synergetic use of industrial solid wastes. Leaching results showed that, the apparent diffusion coefficient values of cesium were only ~1.4×10^{-15} cm^2/s and ~5×10^{-18} cm^2/s at 25 °C and 90 °C leaching conditions, respectively. These values were several orders of magnitude lower when compared with previously reported values, indicating the excellent encapsulation performance of the solid-waste-based SAC for cesium. Moreover, the heavy metals contained in the industrial solid waste were also effectively immobilized. A mechanistic analysis revealed that cesium was encapsulated in the SAC matrices stably by a physical effect. Finally, a life cycle assessment and economic analysis indicated that this approach was environmental-friendly, cost-effective, and energy-saving. This work provides a promising strategy for effective encapsulation of cesium and synergetic treatment of industrial solid wastes.

Keywords: Cesium; Sulfoaluminate matrix; Industrial solid wastes; Encapsulation; Environmental-friendly

1 Introduction

The safe and harmless disposal of continuously growing nuclear wastes has

42   become an unavoidable problem in the field of energy and environment[1,2]. Take

43   Europe as an example, the estimated amount of nuclear waste in European nuclear

44   facilities during the lifetime of a given reactor is even greater than 6.6 million m^3[3].

45   Radioactive cesium (Cs) is one of the most problematic radionuclides contained in

46   nuclear wastes, owing to its high volatility, high mobility and relatively long half-life

47   of approximately $\sim$ 30 years[4]. Although extensive studies have been conducted to

48   understand how to reduce the leachability of radioactive Cs from commonly used

49   Portland cement (PC) matrices, relatively high leaching rates are still reported,

50   especially as the leaching temperature increases[5-8]. Considering the serious

51   environmental impacts of radioactive Cs[9-11], and its safe, long-term immobilization

52   of radioactive Cs under the exothermic conditions present in the repository[12], it

53   remains extremely urgent to develop more efficient immobilization approaches.

54   Recent studies have found that sulfoaluminate cement (SAC) may be a better

55   matrix than PC for the immobilization of radioactive substances[13-17]. For instance,

56   Sun et al.[14] detected both lower cumulative leaching fractions and leaching rates for

57   Cs while using SAC matrices to treat radioactive resins. Relatedly, Coumes et al.[16]

58   found that blending SAC with PC increased the waste loading of low-level radioactive

59   slurries to 56%, and reduced the number packages produced by a factor of 1.8. The

60   superiority of SAC immobilization is primarily attributed to its main hydration

61   product—ettringite ($3CaO \cdot Al_2O_3 \cdot 3CaSO_4 \cdot 32H_2O$). Ettringite is of particular interest to

62   waste solidification due to its propensity to incorporate mobile ions and produce

63   "crystal interlocking" effect by its needle-like crystal structure[13-18]. However,

64 systematic research into the immobilization characteristics and mechanisms of how

65 SAC interacts with radioactive substances under various conditions remains lacking.

66 Additionally, the shortage of high-grade raw materials for manufacturing SAC along

67 with its high production costs has significantly restricted its production and application,

68 in particular, in nuclear waste treatment[19-21].

69   At the other end of the spectrum, global urban wastes are statistically in the range

70 of 7 to 10 billion tons per annum[22]. However, controlled disposal rates are often well

71 below 50% overall in low-income areas, indicating that innovative resource recovery

72 technology is urgently needed[22]. Previous work from our laboratory showed that the

73 synergetic-complementary use of industrial solid wastes can potentially produce a high-

74 performance SAC[20]. Using this high-performance SAC, products that are

75 economically efficient, environmentally friendly can then be manufactured with great

76 potential for various industrial applications[20,21,23-30]. However, there are few

77 studies that have explored the combination of solid waste-derived SAC matrix and

78 nuclear waste disposal.

79   Presented here is an innovative, technical approach for solidifying nuclear wastes

80 using solid waste-derived SAC. The SAC material was first prepared by synergetic-

81 complementary use of industrial solid wastes, which was then employed to encapsulate

82 a simulated Cs. The leaching kinetics of Cs and the synergetic immobilization

83 characteristics of heavy metals contained in the matrix were investigated. The

84 encapsulation mechanisms of Cs were studied using X-ray diffraction (XRD), X-ray

85 photoelectron spectroscopy (XPS), and electron probe microanalysis (EPMA). Finally,

86 the safety, feasibility, and economics of this approach were assessed by both a life cycle

87 assessment and economic analysis. Collectively, this study showed the coordinated

88 digestion of industrial solid waste and nuclear waste, which supports current trends

89 towards green chemistry and a circular economy.

90 2 Materials and methods

91 2.1 Materials and reagents

92   Cesium nitrate ($CsNO_3$) powder was used as the simulant for radioactive Cs; to

93 prepare it for use in the solidification experiment, it was first dissolved in deionized

94 water according to previously published methods[4,8,31,32]. The chemical reagents

95 used in this study were all of analytical grade and were purchased from Aladdin

96 Biochemical Technology Co., Ltd. De-ionized water was used for the preparation and

97 dilution of all chemical solutions. To prepare SAC, five kinds of industrial solid wastes

98 were used with complementary matching of ingredients. Wastes were obtained as

99 follows: (i) MSWI-FA was obtained from Zichuan Waste Incineration Plant (Shandong,

100 China), (ii) desulfurization gypsum was supplied by Liaocheng Coal-fired Power Plants

101 (Shandong, China), (iii) aluminum dust and (iv) titanium gypsum were both supplied

102 by the XinFa Group (Shandong, China), and (v) carbide slag was obtained from

103 Liaocheng Acetylene Company (Shandong, China). The X-ray fluorescence (XRF) and

104 XRD results for the raw materials are presented in Table S1 and Figure S1, respectively.

105 The concentration distributions of heavy metals in solid wastes are given in Table S2.

106 2.2 Experimental procedure

107   The schematic overview of the investigations carried out in this paper is shown in

108   Figure 1. Briefly, two solid-waste-based SACs (M1 and M2) were first prepared *via* a

109   synergetic-complementary approach (a detailed procedure is provided in Table S3)

110   using the above mentioned industrial solid waste materials. The mineral compositions

111   of M1 and M2 are shown in Figure S2. The prepared SAC was then mixed with $CsNO_3$

112   solution to prepare a mixed paste with a water-to-binder ratio of 0.3. The Cs

113   concentration was fixed at 3% of Cs/hardened paste by mass. The fresh paste was then

114   cast into cylinder molds (internal diameter = 20 mm, and internal height = 18 mm) and

115   de-molded after 24 h. The de-molded cylinder sample was cured at 95% humidity and

116    $20 \pm 2°C$ for 28 d before the leaching test. The leaching test was conducted according

117   to ANSI/ANS-16.1- 2003[31,33], and the leaching intervals were set at 2 h, 7 h, 24 h,

118   2 d, 3 d, 4 d, 5 d, 19 d, 47 d, and 90 d. The leaching characteristics of Cs and the heavy

119   metals from different SAC matrices (M1 and M2) at different leaching temperatures

120   (25°C and 90°C) were then investigated. It should be noted that 90°C was employed

121   here to simulate the high temperature which could potentially occur during the decay

122   of radionuclides in the nuclear waste repository.
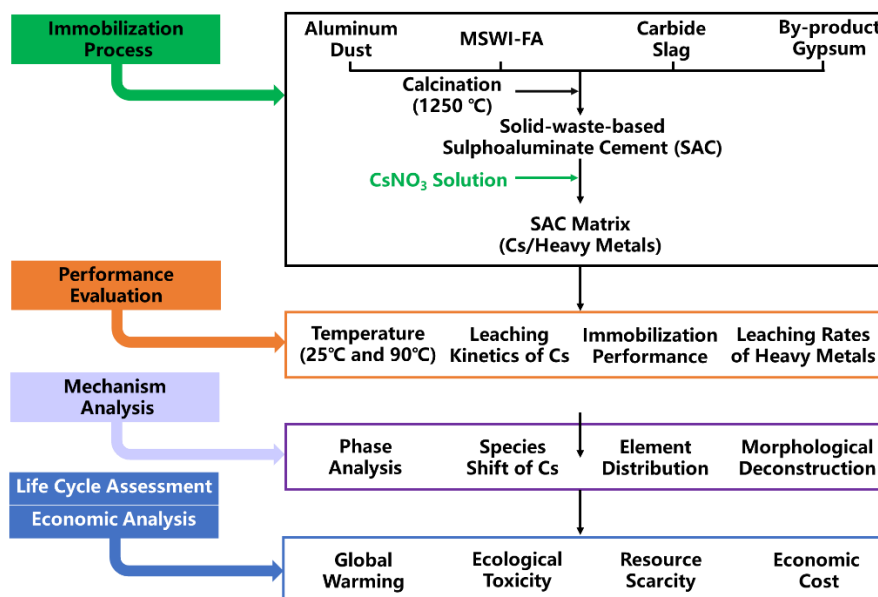
123

124   **Figure 1.** Schematic overview of the investigations undertaken in this study

125 **2.3 Method of evaluating cesium encapsulation**

126   To measure the long-term leaching behavior of Cs, cumulative leaching fraction

127 (CLF) and leaching rate (LR) were calculated according to the equations defined in the

128 literature as shown below in Eq. (1) and Eq. (2), respectively[14].

129
$$CLF = \left(\frac{\sum A_n}{A_0}\right)\left(\frac{V}{S}\right) \qquad (1)$$

130
$$LR = \left(\frac{A_n}{A_0}\right)\left(\frac{V}{S}\right)\left(\frac{1}{t_n}\right) \qquad (2)$$

131   In addition, apparent diffusion coefficient (D) is calculated according to Eq. (3)

132 which could potentially be used to predict the long-term leaching behavior of Cs[14].

133
$$D = \pi \left(\frac{mV}{2S}\right)^2 \qquad (3)$$

134 where A_n is the mass of leached Cs at the nth interval, mg; A_0 is the total original

135 mass of Cs in the specimen, mg; V is the volume of the specimen, cm^3; S is the

136 surface area of the specimen, cm^2; t_n is the duration of the nth interval, d; m is the

137 slope of the straight line of the plot of ($\sum A_n/A_0$) versus (t_n)$^{1/2}$.

138 **2.4 Analytical methods**

139   The mass concentrations of Cs and 8 heavy metals (As, Zn, Pb, Cd, Ni, Mn, Cr,

140 and Cu) in the leachates were determined using an inductively coupled plasma optical

141 emission spectroscopy (ICP-OES; PerkinElmer Optima 7000DV, PE, USA). The pH

142 values of all collected leachates at the end of each leaching interval were determined

143 using a conventional pH analyzer (PHS-25, Lei-ci, China). The mineral phases of Cs-

144 doped samples, raw materials, SAC clinkers and SAC hydration products were

145 characterized by X-ray diffraction (XRD; Rigaku Dmax-2500 PC, Rigaku, Japan) using

146 Cu-Ka radiation with 50 kV voltage, 100 mA current, and a scanning speed of 2.4º/min

147 over a range of 5º-65º. The morphologies and structures of Cs-doped samples were

148 characterized with scanning electron microscopy coupled with an energy dispersive

149 spectrometer (SEM/EDS; Zeiss Supra 55, Carl Zeiss MERLIN Compact, Germany).

150 The chemical shift of Cs in the Cs-doped samples was analyzed using an X-ray

151 photoelectron spectroscopy analyzer (XPS; AXIS Supra, Shimadzu, Japan). The

152 distributions of Cs and heavy metals in the Cs-doped samples were then characterized

153 using a field emission electron probe microanalyzer (FE-EPMA; JXA-8530F Plus,

154 JEOL, Japan). Life cycle assessment was conducted using SimPro ReCiPe2016 H 1.01

155 model.

3 Results and discussion

3.1 Leaching characteristics and kinetics of cesium

158 As shown in Figure 2a, the cumulative leaching fraction (CLF) values of Cs^+ at 90

159 d for M1-25°C, M2-25°C, M1-90°C, and M2-90°C were 1.20×10^{-4} cm, 1.19×10^{-4} cm,

160 7.26×10^{-6} cm, and 7.06×10^{-6} cm, respectively. The CLF values presented here were

161 much lower than the required value of 4×10^{-3} cm as per the GB 14569.1-2011 (Chinese

162 standard for cement waste form)[34,35]. This result indicates that the solid-waste-based

163 SAC has a good effect on immobilizing Cs which can satisfy the requirements for

164 industrial applications. In addition, M2 showed a better immobilizing effect on Cs,

165 which had higher compressive strengths than M1 (as shown in Table S4). This finding

166 implies that high mechanical strength is beneficial to the encapsulation of Cs. Notably,

167 the CLF values at 90 °C condition were two orders of magnitude lower than those at

168   the 25 °C condition.
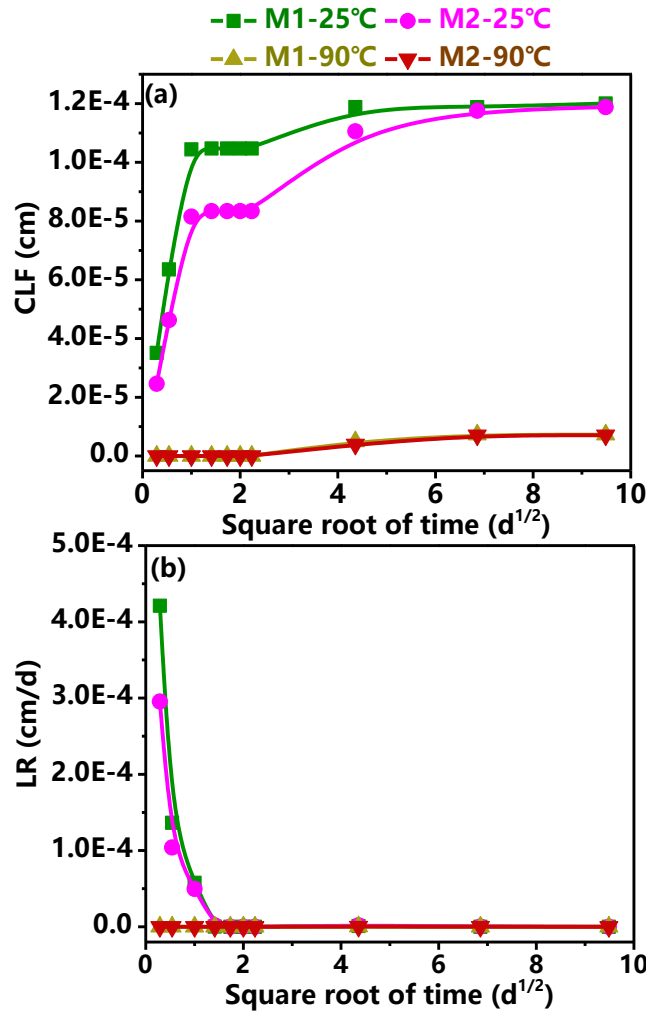
Figure 2. (a) Cumulative leaching fraction, (b) Leaching rate of Cs from the SAC

matrices

As shown in Figure 2b, the leaching of Cs at 25°C mainly occurred on the first

day, with the leaching rate (LR) values decreasing quickly in subsequent time points.

However, a small amount of Cs also leached beyond day 5. In contrast, no Cs leaching

was detected in the first five days at 90°C condition; moreover, the LR values

remained at very low levels during the entire leaching test. Although Cs leaching was

detected from days 19-47, the overall leaching amount remained very low.

178   Based on the results presented in Figure 2, it can be concluded that when the SAC

179   matrix was leached at 25°C, an initial fast leaching of Cs occurred during the first period

180   followed by a slow leaching in subsequent periods. However, when the SAC matrix

181   was leached at 90°C, a slow leaching of Cs was observed during entire periods.

182   Given these findings, the leaching patterns are divided into two regions: Region I

183   (2 h-1 d) and Region II (5-90 d). According to work reported in the literature[6], the

184   controlling leaching mechanism is determined by the slope (k) of the linear regression

185   of $log\,CLF$ versus $log\,t$ (Table S5), with lower k values reflecting lower leaching.

186   In terms of the leaching at 25°C, the k values for Regions I and II were 0.35-0.65 and

187   less than 0.35, respectively. These findings indicated that the corresponding mechanism

188   of Cs leaching from the studied matrices was a diffusion mechanism and a surface

189   wash-off mechanism, respectively[6,14]. In the case of leaching at 90°C, the k values

190   for Region II were less than 0.35, indicating the surface wash-off mechanism dominated

191   the leaching of Cs[6,14]. These results implies that even at 90°C the SAC matrices

192   could still maintain a good encapsulation of Cs.

193 3.2 Encapsulation performance on cesium

194   Numerous researches have studied the Cs leachability from various matrices,

195   including PC, SAC, alkali-activated blends (AABs), and geopolymer[5-7,14,31,36-39].

196   Previous studies evaluated the leaching behavior of nuclides from different matrices by

197   calculating the apparent diffusion coefficient (D) using Fick's second law[5,36], where

198   lower D values are related to reduced leaching of Cs from the matrices.

199
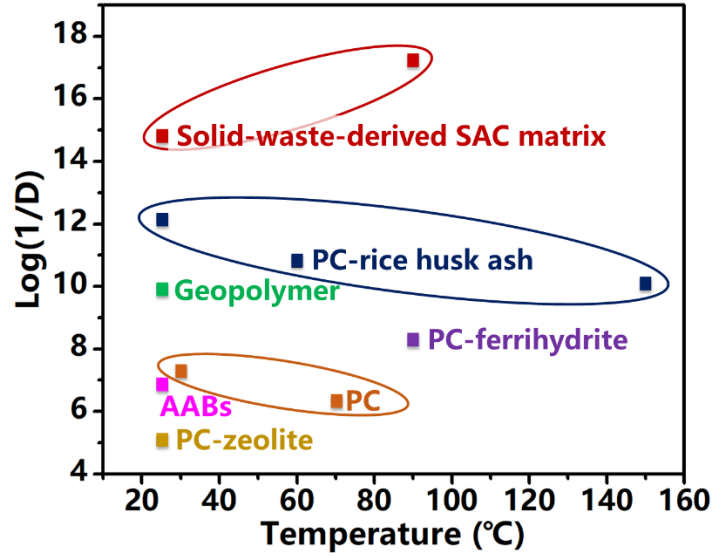
Figure 3. Comparison of Cs encapsulation performance of the SAC matrix in

this work and the various matrices in previous literatures

To intuitively compare the Cs encapsulation performance of the mentioned

matrices, the logarithm of the fractional number of the D values reported in previous

studies and those obtained in current work were calculated using Eq. (3) and plotted

together in Figure 3. As presented, the D values of Cs for M1-25°C, M2-25°C, M1-

90°C, and M2-90°C were calculated to be 1.45×10^{-15} cm^2/s, 1.42×10^{-15} cm^2/s, $5.33 \times$

10^{-18} cm^2/s, and 5.05×10^{-18} cm^2/s, respectively. The calculated values of the solid-

waste-based SAC in this work are obviously higher than other materials. This result

showed that the D values in this study were several orders of magnitude lower when

compared with previously reported values despite the different leaching test conditions.

Therefore, the solid-waste-based SAC has clearly demonstrated its capacity in

improving the encapsulation performance on Cs as compared with other studied

materials.

As shown in Figure 3, the Cs encapsulation performance of PC-based matrices

11

215 decreased as the test temperature increased. In El-Dakroury et al.'s study[7], the *D*

216 values increased from 6.3×10^{-13} cm^2/s to 8.1×10^{-11} cm^2/s when the leaching

217 temperature changed from 25℃ to 150℃. Similar results were also obtained in

218 Papadokostaki et al.'s study on investigating the leachability of Cs from PC-based

219 matrices at different temperatures[5]. However, in the current work, the *D* values

220 decreased by three orders of magnitude as the temperature changed from 25℃ to 90℃,

221 representing a significant reduction in the leaching of Cs. Therefore, it could tentatively

222 conclude that the solid-waste-based SAC could be a suitable for treating Cs containing

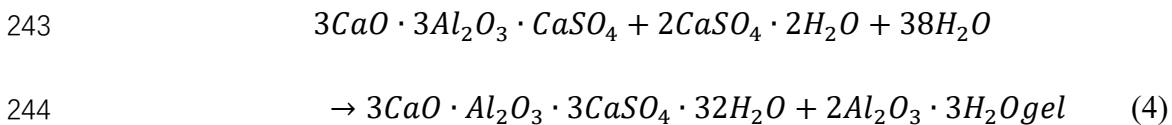223 wastes at high temperature conditions.

224 3.3 Mechanism for cesium encapsulation

225 Figure 4 presents the XRD patterns of Cs-doped samples containing different

226 amounts of Cs at the age of 3 days. It should be noted that higher contents of Cs were

227 doped in these samples in an attempt to facilitate the understanding of the encapsulation

228 mechanisms involved with SAC matrices. The XRD results showed that the appearance

229 of the diffraction peaks of E and Y which could be attributed to the hydration of SAC

230 (Eq. (4)). With the increasing Cs, the main diffraction peaks of CsNO$_3$ became obvious.

231 No other new peaks appeared, which indicated that the incorporation of Cs in SAC

232 might be a physical effect. This hypothesis could be well corroborated by the study

233 reported by R.O.Abdel Rahman et al.[40], in which they found that Cs existed as free

234 ions in the interstitial pore fluid as well as in the intermolecular channels in ettringite

235 and C-S-H structures, contributing to the physical entrapment of Cs within the cement–

236 bentonite matrices. The XPS spectra of Cs (Figure S3) indicated that Cs also did not

undergo any chemical shifts during the SAC hydration process (1h - 3d). This finding

confirmed that the incorporation of Cs in the SAC-based matrix could be a physical

effect.
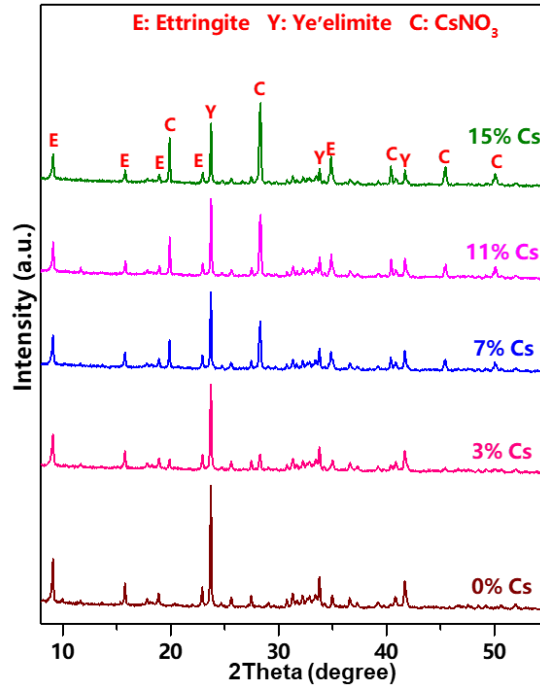
Figure 4. XRD patterns of Cs-doped samples containing different amounts of Cs at 3d

hydration period

$$3CaO \cdot 3Al_2O_3 \cdot CaSO_4 + 2CaSO_4 \cdot 2H_2O + 38H_2O$$

$$\rightarrow 3CaO \cdot Al_2O_3 \cdot 3CaSO_4 \cdot 32H_2O + 2Al_2O_3 \cdot 3H_2O\,gel \qquad (4)$$

The influence of temperature on the Cs encapsulation process was explored

(Figure 5a and Figure 5b). As shown in Figure 5a, remained ye'elimite

($3CaO \cdot 3Al_2O_3 \cdot CaSO$, $C_4A_3\hat{S}$) and gypsum in the initial Cs-doped sample have hydrated

to form ettringite after 90d leaching test at 25°C. The needle-like and prismatic structure

of ettringite in the samples after leaching test at 25°C condition is shown in Figure S4.

Past work has implicated this structure as a causal agent in crystal interlocking[41],

reducing permeability and enhancing the ion encapsulation effects of the matrices.

13

252 Therefore, the leaching rates of Cs at the 25°C leaching condition decreased rapidly

253 during the first day, and gradually decreased even further from day 1 to 90. The EDS

254 data of Cs in Figure S4 also implied that there was almost no selectivity in the

255 encapsulation positions of Cs in the solid-waste-based SAC.

256
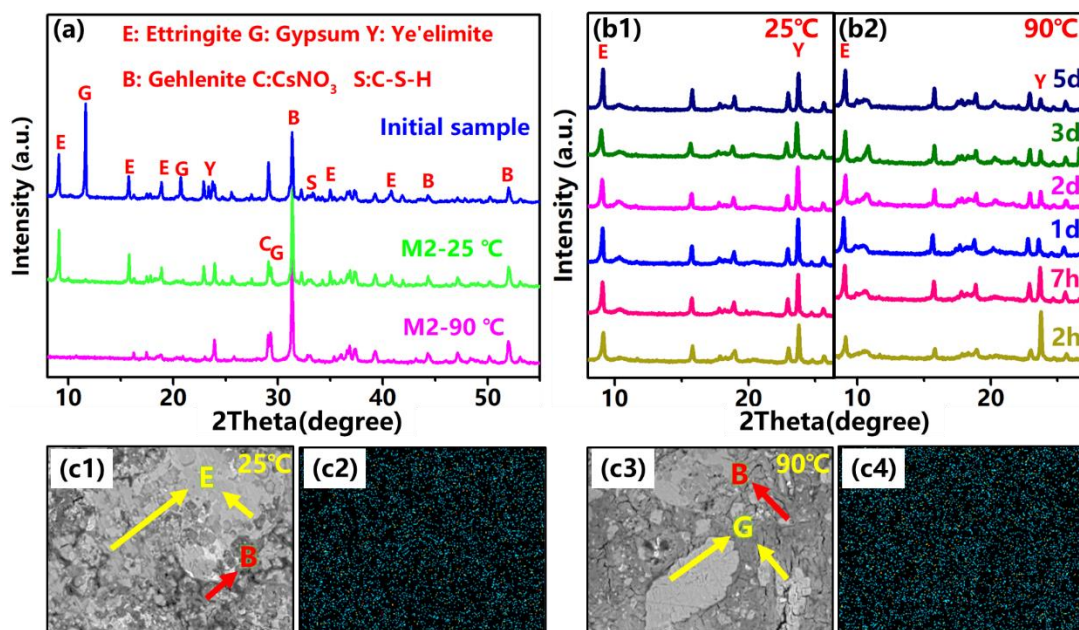
Figure 5. (a) XRD patterns of M2 samples before and after leaching test; (b) XRD

258 patterns of SAC samples curing at 25°C and 90 °C conditions; (c) EPMA mapping of

259 M2 samples after leaching test

260 Compared with Figure 5b1, the peaks of ye'elimite in Figure 5b2 were notably

261 decreased from 2 h to 5 d at the 90°C leaching condition, indicating further hydration

262 of ye'elimite. Past work has also confirmed that increasing curing temperature can

263 promote ye'elimite hydration[42-44]. The higher early-age pH values (9.5-12) of the

264 leachates at the 90°C leaching condition compared to those (7.7-11) at the 25°C

265 leaching condition (Figure S5) also implied the rapid hydration speed of ye'elimite at

266 the 90°C leaching condition. Meanwhile, C–S–H density in the samples was increased

267   with its ongoing hydration at elevated temperatures[45], and its polymerization was

268   increased[46]. Taken together, these results indicated the low leaching of Cs at the early

269   stage of the 90°C leaching condition.

270   However, the ettringite peaks were notably decreased and disappeared after 90d

271   leaching test at 90°C. Previous study found that, ettringite started to convert to AFm

272   ($3CaO \cdot Al_2O_3 \cdot CaSO_4 \cdot 12H_2O$, monosulfoaluminate) and converted to gypsum and an

273   amorphous phase containing aluminum[47]. The backscattered electron images (Figure

274   5c1 and Figure 5c3) and SEM/EDS results (Figure S4) indicated that, ettringite in the

275   Cs-doped samples decomposed at the 90°C condition, and the remained minerals were

276   mainly gypsum, amorphous phase containing aluminum, some traces of AFm and C-S-

277   H gel. This result is consistent with those from previous studies which showed that

278   ettringite was unstable and decomposed at high temperatures[48-50]. However, it seems

279   the phase change of ettringite did not influence the distribution characteristics of Cs in

280   the samples (Figure 5c2 and Figure 5c4). The remained C-S-H and decomposition

281   products of ettringite probably contributed to the subsequent encapsulation of Cs in

282   SAC-based matrices at 90°C leaching condition.

283 **3.4 Synergetic immobilization effect on incorporated heavy metals**

284   To investigate the synergetic immobilization effects of heavy metals by the solid-

285   wastes-based SAC during the leaching tests, the mass concentrations of heavy metals

286   in the leachates were analyzed (Figure 6). Generally, the M2 matrixes—with its higher

287   compressive strength when compared with M1—had lower leaching of heavy metals.

288   The leached Cr and As concentrations were notably higher at the 90°C condition;

289 comparatively, the leaching concentrations of Ni and Mn were slightly higher at the

290 25°C condition. The leaching concentrations of Cu were not affected by leaching

291 temperature; no leached Zn was detected in the early stage at both the 25°C and 90°C

292 conditions.
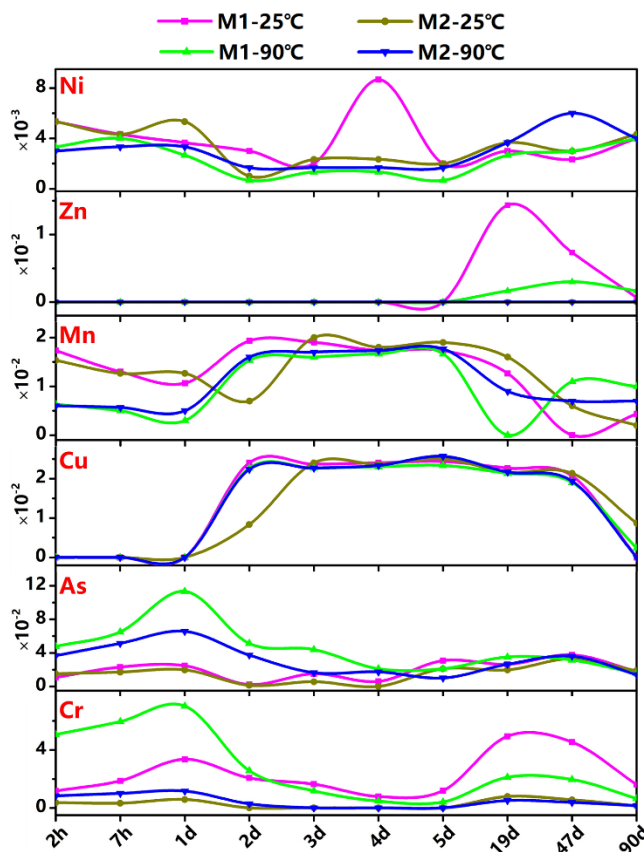
294 **Figure 6.** Mass concentrations of heavy metals in the leachates (mg/L)

295 The leaching concentrations of Zn, Mn, As, Ni, and Cu at the 25°C and 90°C

296 conditions were all much lower than the limits specified in the Chinese integrated

297 wastewater discharge standard GB 8978, U.S. EPA TCLP guidelines, and European

298 landfill directive for non-hazardous waste (Table S6)[51,52]. The leaching

299 concentrations of Cr at the 90°C condition were higher than the GB 8978 limit (1.5

300 mg/L), but lower than the European directive limit (10 mg/L). The leaching

301 concentrations of Cr at 25°C condition were below the limits referenced in the above

302   standards. The EPMA element mapping images of the minerals in the Cs-doped samples

303   (Figure S6) showed that most elements were enriched in the interstices or tightly

304   combined with elemental Ca or Al. In summary, these results indicated that the solid-

305   waste-based SAC had an efficient and synergetic immobilization effect on most heavy

306   metals. Critically, this effect was observed at both high and low temperature conditions.

307   Cr, Zn, and Mn were the most abundant heavy metals in the solid wastes derived

308   SAC clinkers, which accounted for 1348.3 mg/kg, 826.7 mg/kg, 871.3 mg/kg in M1

309   clinker and 181.0 mg/kg, 925.6 mg/kg, 405.5 mg/kg in M2 clinker, respectively. As

310   shown in Figure S6, most elements of Mn and Zn were enriched in the interstices of

311   Ca- or Al- containing minerals both at 25℃ and 90℃ conditions, despite of the

312   chemical change of ettringite. These elements were probably incorporated in the SAC

313   clinker during the calcination process and hardly participated in hydration

314   reaction[53,54], which explained the low leaching of Zn and Mn during the leaching

315   tests. Most elements of Cr were enriched in the interstices of the Ca-containing minerals

316   at 25℃ condition, but they became evenly distributed in the sample leached at 90℃

317   condition. The decomposition of ettringite at 90℃ condition might have led to the

318   release and migration of Cr owing to its high mobility[55]. These results indicated that,

319   the phase transition of SAC clinkers had different effects on the immobilization and

320   migration of various heavy metals.

321   **3.5 Life cycle assessment and economic analysis**

322   Figure 7a contains a simplified flow chart of the production of solid-waste-based

323   SAC, traditional SAC and PC. Compared with traditional SAC and PC, there are clear

324 advantages of producing SAC *via* synergetic-complementary use of industrial solid

325 wastes, including: (1) reduced raw material costs and energy consumption, (2)

326 extensive consumption of industrial solid wastes, and (3) products with high-

327 performance. These features are all associated with potential environmental and

328 economic benefits that can be analyzed *via* life cycle assessment and economic analysis.
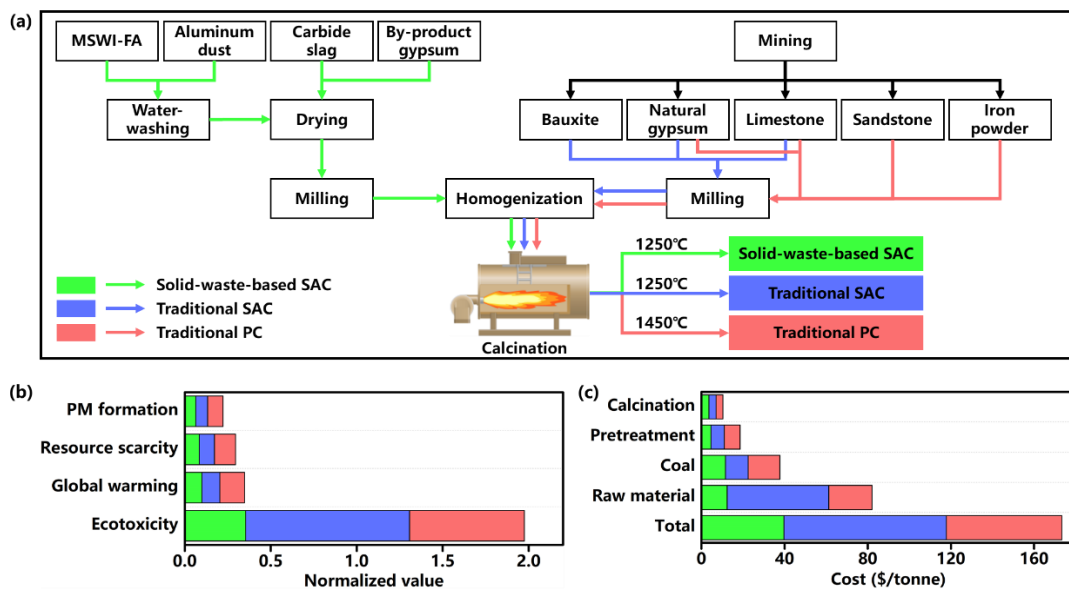
329

330 **Figure 7.** Environmental and economic analyses of the production of solid-waste-based

331 SAC, traditional SAC and PC: (a) Simplified flow chart; (b) Major environmental

332 impacts in LCA results; (c) Production costs

333   The three different cements are then modeled assuming that 1 tonne of clinker was

334 produced for each cement type. The normalization results (Figure 7b) revealed that the

335 four major environmental impacts were ecotoxicity, global warming, resource scarcity,

336 and PM formation. The normalized value of ecotoxicity to produce the solid-waste-

337 based SAC was 62.7% and 46.9% lower than that for traditional SAC and PC,

338 respectively, indicating that the technical route in this work is much more

339 environmentally-friendly.

18

340   Greenhouse gas emission is also an important factor to consider. As shown in

341   Figure 7b, the global warming value resulting from the solid-waste-based SAC

342   production was only 69.5% of that for traditional PC. Moreover, the resource scarcity

343   value for the solid-waste-based SAC was 3.4% and 30.6% lower than that for traditional

344   SAC and PC, respectively. Moreover, the mineral resource scarcity value was only 0.07%

345   and 0.2% that for traditional SAC and PC, respectively. Collectively, these results

346   demonstrated the lower total energy and mineral resource consumption in the

347   production of solid-waste-based SAC. In addition, the PM formation from the solid-

348   waste-based SAC was also lower than that for traditional SAC and PC. Detailed LCA

349   results are provided in the Supporting Information (Figure S7).

350   Production costs were also analyzed; results are shown in Figure 7c. The total

351   production costs for the solid-waste-based SAC, traditional SAC, and PC were $39.7,

352     $78.0, and $55.6 per tonne, respectively. We also observed that the low cost of the raw

353   materials was a key factor in the total cost reduction for the solid-waste-based SAC

354   relative to traditional SAC and PC. Moreover, the cost of water-washing and heating

355   pretreatment process for MSWI-FA and aluminum dust was only $2.3, which did not

356   cause a significant increase in total cost. Detailed economic analysis results are

357   provided in Table S7.

358   These results indicated that SAC production using industrial solid wastes achieved

359   environmentally friendly nature and large-scale resource utilization of solid wastes.

360   Moreover, their production was associated with significant reductions in the overall

361   environmental burden compared to the traditional approaches[28]. The production cost

of solid-waste-based SAC was much lower than that of either traditional SAC or PC, especially in terms of raw material costs. Moreover, solid-waste-based SAC promotes the comprehensive utilization of industrial solid wastes through a circular development approach[21].

3.6 Environmental implications

The safe use of cleaner nuclear energy significantly reduces the consumption of fossil fuels, thereby improving energy efficiency and ensuring a sustainable supply of energy for human society. However, the safe disposal of nuclear waste is an environmental and energy-related problem that the world must face and solve. One such solution to this problem is to use industrial solid wastes to synthesize green materials; these materials are then used for nuclear waste solidification. This approach allows for the safe and cost-effective disposal of nuclear wastes, while also solving the problem of high-value industrial solid waste utilization. Ultimately, it is a sound strategy with great industrial prospects and potential applications. The solid-waste-based SAC matrix prepared in this study exhibited excellent solidification effects on Cs and heavy metals from the perspective of long-term solidification. The technical route has the potential to promote the substantial development of nuclear power and the large-scale utilization of solid wastes; moreover, this approach also promotes the construction of a new industrial chain. Collectively, this work provides a promising pathway to realize the solidification of nuclear wastes and synergetic treatment of industrial solid wastes.

4 Conclusions

The solid waste-derived sulfoaluminate matrix exhibited very effective

384 encapsulation performance for cesium, as well as for the heavy metals introduced from

385 industrial solid wastes. Especially, the cumulative leaching fraction values of cesium at

386 90 ℃ condition were two orders of magnitude lower than those of 25 ℃ condition,

387 indicating the better encapsulation performance of the solid waste-derived

388 sulfoaluminate matrix at high temperature.

389   The solidification mechanism of cesium in the studied matrix was found to be a

390 physical encapsulation. The increase of temperature could accelerate the hydration of

391 the remained ye'elimite in the matrices and promote the formation of ettringite, which

392 might contribute to the much lower leaching of cesium at the early stage of the 90 ℃

393 condition than that at the 25 ℃ condition. Despite the decomposition of ettringite at

394 90 ℃ condition after long-term leaching test, the phase change of ettringite did not

395 influence the effective encapsulation of cesium.

396   The production of solid waste-derived sulfoaluminate matrix could achieve

397 environmentally friendly nature and large-scale resource utilization of industrial solid

398 wastes. This approach of treating nuclear wastes with solid wastes allows for the safe

399 and cost-effective disposal of nuclear wastes, while also help to promote the high-value

400 utilization of industrial solid wastes.

401 **Supporting information**

402 XRD patterns of raw materials (**Figure S1**); XRD patterns of M1 and M2 clinkers

403 (**Figure S2**); XPS spectra of 3% Cs-doped samples hydrated for different durations up

404 to 3d (**Figure S3**); SEM/EDS results of the Cs-doped samples after 90d leaching test

405 (**Figure S4**); pH values of leachates at different time (**Figure S5**); EPMA element

mapping images of the minerals in M2 samples after leaching tests (**Figure S6**); LCA

results for production of solid-waste-based SAC, traditional SAC and PC (**Figure S7**);

Chemical compositions of solid waste raw materials (**Table S1**); Concentrations of 8

heavy metals in raw materials and prepared SAC (**Table S2**); Proportions of the solid

waste samples in raw meals (**Table S3**); Compressive strengths and setting times of M1

and M2 pastes (**Table S4**); k values for controlling leaching mechanism (**Table S5**);

Concentrations of heavy metals in different leachate (mg/L) (**Table S6**); Economic

comparison of the production of solid-waste-based SAC, traditional SAC and PC

(Table S7).

Author information

Corresponding author

Wenlong Wang*

Address: No.17923 Jingshi Road, Shandong University, Jinan City 250014, China

Tel.: +86-531- 88399372

E-mail: wwenlong@sdu.edu.cn

Notes

The authors declare no competing financial interest.

Acknowledgements

References:

[1] Q. Huang, F. Wang, Z. Huang, Y. Yang, L. Li, Key Issues and Countermeasures on Environmental

431   Risk Prevention and Control of Hazardous Wastes, Research of Environmental Sciences, 31 (2018)
432   789-795.

433 [2] S. Ji, Y. Li, S. Ma, C. Liu, K. Shih, C. Liao, Synergistic effects of Ln and Fe Co-Doping on phase
434   evolution of $Ca_{1-x}Ln_xZrTi_{2-x}Fe_xO_7$ (Ln = La, Nd, Gd, Ho, Yb) ceramics, J NUCL MATER, 511
435   (2018) 428-437.

436 [3] A. Jungjohann, M. Besnard, M. Buser, I. Fairlie, G. MacKerron, A. Macfarlane, E. Matyas, Y.
437   Marignac, E. Sequens, J. Swahn, B. Wealer, World Nuclear Waste Report 2019. Focus Europe,
438   2019.

439 [4] J. Li, D. Xu, W. Wang, X. Wang, Y. Mao, C. Zhang, W. Jiang, C. Wu, A. Serikov, Review on
440   Selection and Experiment Method of Commonly Studied Simulated Radionuclides in Researches
441   of Nuclear Waste Solidification, SCI TECHNOL NUCL INS, 2020 (2020) 3287320.

442 [5] K.G. Papadokostaki, A. Savidou, Study of leaching mechanisms of caesium ions incorporated in
443   Ordinary Portland Cement, J HAZARD MATER, 171 (2009) 1024-1031.

444 [6] R.O. Abdel Rahman, A.A. Zaki, A.M. El-Kamash, Modeling the long-term leaching behavior of
445   ^{137}Cs, ^{60}Co, and ^{152,154}Eu radionuclides from cement‒clay matrices, J HAZARD MATER, 145
446   (2007) 372-380.

447 [7] A. El-Dakroury, M.S. Gasser, Rice husk ash (RHA) as cement admixture for immobilization of
448   liquid radioactive waste at different temperatures, J NUCL MATER, 381 (2008) 271-277.

449 [8] G. Bar-Nes, A. Katz, Y. Peled, Y. Zeiri, The mechanism of cesium immobilization in densified
450   silica-fume blended cement pastes, CEMENT CONCRETE RES, 38 (2008) 667-674.

451 [9] X.J. Wang, H.Y. Xiao, X.T. Zu, W.J. Weber, Study of cerium solubility in $Gd_2Zr_2O_7$ by DFT + U
452   calculations, J NUCL MATER, 419 (2011) 105-111.

453 [10] Y. Yang, X. Wang, S. Luo, X. Yang, J. Ma, Stability studies of $[Cs_xBa_y][(Al^{3+},Ti^{3+})_{(2y+x)}Ti^{4+}_{8-2y-x}]O_{16}$ ceramics for radioactive caesium immobilization, CERAM INT, 45 (2019) 7865-7870.
454

455 [11] X. Liu, J. Wu, L. Hou, J. Wang, Removal of Co, Sr and Cs ions from simulated radioactive
456   wastewater by forward osmosis, CHEMOSPHERE, 232 (2019) 87-95.

457 [12] Y. Xu, X. Xue, L. Dong, C. Nai, Y. Liu, Q. Huang, Long-term dynamics of leachate production,
458   leakage from hazardous waste landfill sites and the impact on groundwater quality and human
459   health, WASTE MANAGE, 82 (2018) 156-166.

460 [13] J. Li, Z. Gang, J. Wang, Solidification of low-level-radioactive resins in ASC-zeolite blends,
461   Nuclear Engineering & Design, 235 (2005) 817-820.

462 [14] Q. Sun, J. Li, J. Wang, Solidification of borate radioactive resins using sulfoaluminate cement
463   blending with zeolite, Nuclear Engineering & Design, 241 (2011) 5308-5315.

464 [15] S. Peysson, J. Péra, M. Chabannet, Immobilization of heavy metals by calcium sulfoaluminate
465   cement, Cement & Concrete Research, 35 (2005) 2261-2270.

466 [16] C.C.D. Coumes, S. Courtois, S. Peysson, J. Ambroise, J. Pera, Calcium sulfoaluminate cement
467   blended with OPC: A potential binder to encapsulate low-level radioactive slurries of complex
468   chemistry, Cement & Concrete Research, 39 (2009) 740-747.

469 [17] Q. Zhou, N.B. Milestone, M. Hayes, An alternative to Portland Cement for waste encapsulation—
470   The calcium sulfoaluminate cement system, J HAZARD MATER, 136 (2006) 120-129.

471 [18] A. Telesca, M. Marroccoli, M.L. Pace, M. Tomasulo, G.L. Valenti, P.J.M. Monteiro, A hydration
472   study of various calcium sulfoaluminate cements, Cement and Concrete Composites, 53 (2014)
473   224-232.

474 [19] J. Li, W. Wang, D. Xu, X. Wang, Y. Mao, Preparation of sulfoaluminate cementitious material using

harmful titanium gypsum: material properties and heavy metal immobilization characteristics, Waste Disposal & Sustainable Energy, 2 (2020) 127-137.

[20] C. Ren, W. Wang, G. Li, Preparation of high-performance cementitious materials from industrial solid waste, CONSTR BUILD MATER, 152 (2017) 39-47.

[21] C. Ren, W. Wang, Y. Mao, X. Yuan, Z. Song, J. Sun, X. Zhao, Comparative life cycle assessment of sulfoaluminate clinker production derived from industrial solid wastes and conventional raw materials, J CLEAN PROD, 167 (2017) 1314-1324.

[22] J.A.M. Sepúlveda, D.C. Wilson, L. Rodic, P. Modak, R. Soos, A.C. Rogero, C. Velis, M. Iyer, O. Simonett, Global Waste Management Outlook 2015, 2015.

[23] W. Wang, P. Wang, C. Ma, Z. Luo, Calculation for Mineral Phases in the Calcination of Desulfurization Residue to Produce Sulfoaluminate Cement, IND ENG CHEM RES, 49 (2010) 9504-9510.

[24] W. Wang, X. Wang, J. Zhu, P. Wang, C. Ma, Experimental Investigation and Modeling of Sulfoaluminate Cement Preparation Using Desulfurization Gypsum and Red Mud, IND ENG CHEM RES, 52 (2013) 1261-1266.

[25] W. Wenlong, C. Xiaodong, C. Ying, Calculation and Verification for the Thermodynamic Data of $3CaO \cdot 3Al_2O_3 \cdot CaSO_4$, CHINESE J CHEM ENG, 19 (2011) 489-495.

[26] X. Yao, W. Wang, M. Liu, Y. Yao, S. Wu, Synergistic use of industrial solid waste mixtures to prepare ready-to-use lightweight porous concrete, J CLEAN PROD, 211 (2019) 1034-1043.

[27] S. Wu, W. Wang, C. Ren, X. Yao, Y. Yao, Q. Zhang, Z. Li, Calcination of calcium sulphoaluminate cement using flue gas desulfurization gypsum as whole calcium oxide source, CONSTR BUILD MATER, 228 (2019) 116676.

[28] Y. Mao, H. Wu, W. Wang, M. Jia, X. Che, Pretreatment of municipal solid waste incineration fly ash and preparation of solid waste source sulphoaluminate cementitious material, J HAZARD MATER, 385 (2020) 121580.

[29] Q. Shahzad, X. Wang, W. Wang, Y. Wan, G. Li, C. Ren, Y. Mao, Coordinated adjustment and optimization of setting time, flowability, and mechanical strength for construction 3D printing material derived from solid waste, CONSTR BUILD MATER, 259 (2020) 119854.

[30] Z. Ge, H. Yuan, R. Sun, H. Zhang, W. Wang, H. Qi, Use of green calcium sulphoaluminate cement to prepare foamed concrete for road embankment: A feasibility study, CONSTR BUILD MATER, 237 (2020) 117791.

[31] S. Fan, B. Cao, N. Deng, Y. Hu, M. Li, Effects of ferrihydrite nanoparticle incorporation in cementitious materials on radioactive waste immobilization, J HAZARD MATER, 379 (2019) 120570.

[32] S.M. Park, J.G. Jang, Carbonation-induced weathering effect on cesium retention of cement paste, J NUCL MATER, 505 (2018) 159-164.

[33] L.G.P.I. American Nuclear Society, Measurement of the Leachability of Solidified Low-Level Radioactive Wastes by a Short-Term Test Procedure, ANSI/ANS-16.1-2003, (2004).

[34] G.B. Liu, B.C. Wang, Y.C. Jiang, R. Zhang, S.Q. Zhan, Outside Barrel Solidification Process With Cement of Mock Waste Activated Carbon After Saturated With Boron Water, He-Huaxue yu Fangshe Huaxue/Journal of Nuclear and Radiochemistry, 40 (2018) 393-399.

[35] L.I. Honghui, Y. Weibing, F. Wendong, Study on proportioning of simulated concentrate liquid cement solidified radioactive waste form and its properties test, Cement, (2015).

[36] J.G. Jang, S.M. Park, H.K. Lee, Physical barrier effect of geopolymeric waste form on diffusivity

24

of cesium and strontium, J HAZARD MATER, 318 (2016) 339-346.

[37] I. Plecas, S. Dimovic, I. Smiciklas, Influence of bentonite and zeolite in cementation of dry radioactive evaporator concentrates, APPL CLAY SCI, 43 (2009) 9-12.

[38] M. Komljenović, G. Tanasijević, N. Džunuzović, J.L. Provis, Immobilization of cesium with alkali-activated blast furnace slag, J HAZARD MATER, 388 (2020) 121765.

[39] M.R. El-Naggar, E.H. El-Masry, A.A. El-Sadek, Assessment of individual and mixed alkali activated binders for solidification of a nuclear grade organic resin loaded with [134]Cs, ^{60}Co and [152+154]Eu radionuclides, J HAZARD MATER, 375 (2019) 149-160.

[40] R.O. Abdel Rahman, E.A.D.H. Zin, H. Abou-Shady, Cesium binding and leaching from single and binary contaminant cement‐bentonite matrices, CHEM ENG J, 245 (2014) 276-287.

[41] S.M. Leisinger, B. Lothenbach, G.L. Saout, R. K Gi, B. Wehrli, C.A. Johnson, Solid Solutions between CrO_4- and SO_4-Ettringite $Ca_6(Al(OH)_6)_2$-$[(CrO4)_x(SO_4)_{1-x}]3*26H_2O$, ENVIRON SCI TECHNOL, 44 (2010) 8983-8988.

[42] P. Wang, N. Li, L. Xu, Hydration evolution and compressive strength of calcium sulphoaluminate cement constantly cured over the temperature range of 0 to 80°C, CEMENT CONCRETE RES, 100 (2017) 203-213.

[43] L. Li, R. Wang, S. Zhang, Effect of curing temperature and relative humidity on the hydrates and porosity of calcium sulfoaluminate cement, CONSTR BUILD MATER, 213 (2019) 627-636.

[44] Y. Zhang, T. Li, W. Feng, Z. Xiong, G. Zhang, Effects of temperature on performances and hydration process of sulphoaluminate cement-based dual liquid grouting material and its mechanisms, J THERM ANAL CALORIM, 139 (2020) 47-56.

[45] B. Lothenbach, T. Matschei, G. Möschner, F.P. Glasser, Thermodynamic modelling of the effect of temperature on the hydration and porosity of Portland cement, CEMENT CONCRETE RES, 38 (2008) 1-18.

[46] T.T.H. Bach, C.C.D. Coumes, I. Pochard, C. Mercier, B. Revel, A. Nonat, Influence of temperature on the hydration products of low pH cements, CEMENT CONCRETE RES, 42 (2012) 805-817.

[47] A. Jimenez, M. Prieto, Thermal Stability of Ettringite Exposed to Atmosphere: Implications for the Uptake of Harmful Ions by Cement, ENVIRON SCI TECHNOL, 49 (2015) 7957-7964.

[48] X. Wang, Z. Pan, X. Shen, W. Liu, Stability and decomposition mechanism of ettringite in presence of ammonium sulfate solution, CONSTR BUILD MATER, 124 (2016) 786-793.

[49] Q. Zhou, E.E. Lachowski, F.P. Glasser, Metaettringite, a decomposition product of ettringite, CEMENT CONCRETE RES, 34 (2004) 703-710.

[50] A. Jiménez, M. Prieto, Thermal Stability of Ettringite Exposed to Atmosphere: Implications for the Uptake of Harmful Ions by Cement, ENVIRON SCI TECHNOL, 49 (2015) 7957-7964.

[51] X. Liu, X. Zhao, H. Yin, J. Chen, N. Zhang, Intermediate-calcium based cementitious materials prepared by MSWI fly ash and other solid wastes: hydration characteristics and heavy metals solidification behavior, J HAZARD MATER, 349 (2018) 262-271.

[52] K. Wu, H. Shi, X. Guo, Utilization of municipal solid waste incineration fly ash for sulfoaluminate cement clinker production, WASTE MANAGE, 31 (2011) 2001-2008.

[53] N., Gineys, And, G., Aouad, And, F., Sorrentino, And, D., Incorporation of trace elements in Portland cement clinker: Thresholds limits for Cu, Ni, Sn or Zn, Cement & Concrete Research, (2011).

[54] W.L.W.X. Wang Yue, Incorporation Features of Cu^{2+},Zn^{2+},Cr^{6+},Cd^{2+} and Pb^{4+} Ions in Cement Clinker, Bulletin of the Chinese Ceramic Society, (2013) 163-168.

563   [55] S. Bae, F. Hikaru, M. Kanematsu, C. Yoshizawa, J. Ha, Removal of Hexavalent Chromium in

564   Portland Cement Using Ground Granulated Blast-Furnace Slag Powder, MATERIALS, 11 (2018)

565   11.

566

567